IEEE | Transactions on Terahertz Science and Technology

In Situ Hilbert-Transform Spectral Analysis of Pulsed Terahertz Radiation of Quantum Cascade Lasers by High-T_c Josephson Junctions

Journal:	*Transactions on Terahertz Science and Technology*
Manuscript ID	Draft
Manuscript Type:	Regular Paper
Date Submitted by the Author:	n/a
Complete List of Authors:	Volkov, Oleg; Kotelnikov Institute of Radioengineering and Electronics of Russian Academy of Sciences, Physical Electronics Pavlovskiy, Valery; Kotelnikov Institute of Radioengineering and Electronics of Russian Academy of Sciences, , Physical Electronics Gundareva, Irina; Forschungszentrum Jülich GmbH, Peter Grünberg Institute Khabibullin, Rustam; Mokerov Institute of Ultra High Frequency Semiconductor Electronics of Russian Academy of Sciences Divin, Yuriy; Kotelnikov Institute of Radioengineering and Electronics of Russian Academy of Sciences, Physical Electronics; Forschungszentrum Jülich GmbH, Peter Grünberg Institute
TOPIC AREA FOR SUBMISSION :	THz devices and components

In Situ Hilbert-Transform Spectral Analysis of Pulsed Terahertz Radiation of Quantum Cascade Lasers by High-T_c Josephson Junctions

Oleg Volkov, Valery Pavlovskiy, Irina Gundareva, Rustam Khabibullin, and Yuriy Divin

***Abstract*—We have studied the applicability of high-T_c Josephson junctions (JJs) and Hilbert-transform spectral analysis (HTSA) for characterization of pulsed terahertz (THz) radiation. We have reconsidered the extension of HTSA into the THz range, including an impact of such emerging factors as nonequilibrium voltage fluctuations and dc Joule heating in high-T_c JJs, and found an unexpected weak temperature dependence of Josephson linewidth δf and a spectral dependence $\delta f(f)$ with a minimum. Due to this analysis, we have chosen $YBa_2Cu_3O_{7-x}$ bicrystal JJs for experimental study. The JJs have analyzed pulsed THz radiation from quantum cascade lasers (QCLs) located in the same cryogenic environment at 50 K. The spectra recovered by the JJ with R_n = 43 Ω consist of a line with a central frequency around 2.2 THz, which have a symmetrical form and the linewidth of 90 GHz close to the intrinsic Josephson linewidth of this JJ. The spectra measured by the JJ with R_n = 7 Ω and the intrinsic Josephson linewidth of 16 GHz consist of several lines at the frequencies f_i around 2.2 THz, which are due to the excitation of different resonant modes in the active volume of the QCL. The difference between the fitted central frequencies $f_2 - f_1$ of the strong lines and the ratio of their intensities are in agreement with the spectrum of the same QCL measured by Fourier spectroscopy. The developed technique paves the way for detailed and rapid characterization of pulsed THz sources in the frequency domain.**

***Index Terms*—Josephson junctions, high-temperature superconductors, quantum cascade lasers, spectral analysis, terahertz radiation.**

I. Introduction

BRIDGING the terahertz (THz) gap in the electromagnetic spectrum is achieved by extending the frequency ranges of microwave electronics and infrared photonics [1]. Quantum cascade lasers (QCLs) based on InP or GaAs heterostructures deliver very intense radiation in the infrared range [2]. After redesigning these heterostructures to lower spacing between the energy levels, the QCLs demonstrate operation in the frequency range from 1.2 to 5.4 THz [2], [3]. The operating temperatures of continuous-wave (CW) THz QCLs are less than 130 K. Meanwhile, the operation of THz QCLs in pulsed mode allows one to increase the operating temperature up to 210 K [4] and use thermoelectric coolers [4], [5] to widen applications of these radiation sources.

As a rule, Fourier spectroscopy with a Michelson optical interferometer and a low-speed semiconductor detector is the only technique for characterization of the output radiation of pulsed THz QCLs and other radiation sources. This technique is slow due to the mechanical moving of a mirror to get a required difference dx of the beam paths in the interferometer. The maximum path difference δx_{max} determines the frequency resolution $\delta f \cong c/2\delta x_{max}$ of this technique [6].

Heterostructures emit THz radiation in many spatial modes simultaneously with a large spread in directivity. In particular, THz QCLs with double-metal waveguides show highly divergent beams with multiple lobes in the far-field distribution [7]. The angular-resolved spectroscopy shows radiation from the TM_{00} group of the longitudinal modes in the perpendicular direction to the QCL facet and TM_{01} modes at ± 25° to the normal [8]. Fourier spectroscopy cannot simultaneously characterize all these modes because an increase in solid angles of the radiation entering the interferometer leads to the angular-dependent frequency errors (see [6], page 48). Also, significant distortions appear in the harmonic spectra of THz heterostructures due to various phase shifts of the frequency components of the radiation [9].

Given these circumstances, the dynamics, accuracy, and completeness of spectral characterization of any pulsed THz radiation source with Fourier spectroscopy spectral analysis appear to be limited. It looks challenging to find a spectroscopic technique based only on electronic devices and operating in the frequency domain, but not in the phase domain. The proximity of a spectrum analyzer to a radiation source under study may be an added advantage because of higher chances to characterize divergent radiation modes of higher orders. In the case of the

The work was carried out within the framework of the state task of Russian Ministry of Science and High Education. Also, I.G. and Y.D. wish to thank Forschungszentrum Jülich for partial support. The fabrication of THz QCLs was supported by the Russian Science Foundation Grant No. 18-19-00493. (*Corresponding author: Yuriy Divin.*)

O. Volkov and V. Pavlovskiy are with the Kotelnikov Institute of Radio Engineering and Electronics, Russian Academy of Sciences, 125009 Moscow, Russia (e-mail: O_Volkov@cplire.ru and pvv@cplire.ru).

I. Gundareva was with the Peter Grünberg Institute (PGI-5), Forschungszentrum Jülich, 52425 Jülich, Germany, on leave from the Kotelnikov Institute of Radio Engineering and Electronics, Russian Academy of Sciences, 125009 Moscow, Russia. She is now with the Peter Grünberg Institute (PGI-9), Forschungszentrum Jülich, 52425 Jülich, Germany (I.Gundareva@fz-juelich.de).

R. Khabibullin is with the Mokerov Institute of Ultra High Frequency Semiconductor Electronics, Russian Academy of Sciences, 117105 Moscow, Russia (e-mail: khabibullin@isvch.ru).

Y. Divin is with the Kotelnikov Institute of Radio Engineering and Electronics, Russian Academy of Sciences, 125009 Moscow, Russia (e-mail: yyd@cplire.ru) and also with the Peter Grünberg Institute (PGI-5), Forschungszentrum Jülich, 52425 Jülich, Germany (Y.Divin@fz-juelich.de).

measurements with remote Fourier spectrometers, diffraction will additionally weaken these radiation modes.

It looks challenging to find a spectroscopic technique, which is based only on electronic devices operating in the frequency domain, but not in the phase domain. The proximity of a spectrum analyzer to a radiation source under study may be an added advantage because of higher chances to characterize divergent radiation modes of higher orders. These possibilities might come from the application of the ac Josephson effect [10], and the technique of Hilbert-transform spectral analysis (HTSA) [11] might be the best choice. Extension of HTSA into the THz range is possible with the implementation of high-T_c Josephson junctions.

In recent years, several applications of high-T_c Josephson frequency-selective detectors for characterization of THz radiation have been demonstrated [12-17]. Among them are the following: measurements of radiation spectra of various CW polychromatic THz sources [12], [13], [16]; CW broadband radiation from quasiparticle-injected nonequilibrium superconductor [14]; pulsed broadband THz radiation from relativistic electron bunches [15]; and detection of broadband radiation from photoconductive antennas excited by femtosecond optical pulses [17]. Emission of 500GHz-radiation from a $Bi_2Sr_2CaCu_2O_8$ intrinsic Josephson junction has induced multiple Shapiro steps on the *I-V* curves of $YBa_2Cu_3O_7$ grain-boundary junctions [18].

The frequency-selective high-T_c Josephson detectors have been characterized in the THz range, using CW optically pumped gas lasers [19], [20]. The operating frequencies and temperatures of such detectors have broad overlapping regions with similar QCL characteristics. The high-T_c JJs at 10 K demonstrate the highest Josephson frequency of 5.2 THz [20]. These circumstances might be useful for spectral characterization of QCL radiation in the frequency domain when a high-T_c Josephson detector performs spectral analysis in the proximity of the QCL in the same cryogenic environment. In this paper, we present the results of our attempt to characterize pulsed THz QCLs *in situ* using HTSA with high-T_c JJs.

II. Theory

A. Fundamentals of HTSA

The fundamentals of HTSA [11] have been slightly corrected recently [12] and are presented here in a revised form. Briefly, an integral relationship between the detector response $\Delta I(f_j)$ of the Josephson junction to external radiation as a function of the Josephson frequency f_j and the spectrum $S(f)$ of the incident radiation is the basis of the HTSA operation. To recover the spectrum $S(f)$ uniquely, one should apply the inverse Hilbert transform to the measured response $\Delta I(f_j)$ in the following way [11], [12]:

$$S(f) \sim \left(\frac{1}{\pi}\right) P \int_{-\infty}^{+\infty} \frac{H(f_j)df_j}{f_j - f}, \qquad (1)$$

where

$$H(f_j) = \frac{2}{\pi f_c^2} \Delta I(f_j) I_0(f_j) f_j \,, \qquad (2)$$

is the normalized response function, which consists of the product of Josephson frequency $f_j = 2eV/h$, where V is the dc voltage across the junction, the current response $\Delta I(V)$, and the dc $I_0(V)$ curve as the functions of f_j divided by the square of the characteristic Josephson frequency f_c.

When compared with Fourier spectroscopy, Hilbert-transform spectral analysis operates only with a nanoelectronic device, a Josephson junction, and, in principle, is perspective for high-speed measurements. Operation in the frequency domain is among the main distinctive features of HTSA. Besides, due to the principle difference between Fourier and Hilbert transforms, the HTSA is more effective in detecting weak narrowband signals from strong broadband backgrounds than Fourier spectroscopy. More about applications of the HTSA based on high-T_c Josephson junctions to characterization of CW radiation sources with frequencies up to 2.5 THz can be found elsewhere [12].

Application of the HTSA to pulsed radiation is also possible, but thus far only at the sub-THz frequencies [21]. Very low, of the order of 1 ps, characteristic time constants, and extended dynamic power ranges of high-T_c Josephson junctions as radiation detectors have a decisive role in such applications. The dynamic power range $D = P_s/\mathrm{NEP}$ is the ratio of the maximum power value P_s, where the detector response deviates from the linear dependence by less than 1 dB, and the value of Noise Equivalent Power (NEP) in $\mathrm{W/Hz^{1/2}}$ calculated for the output detector bandwidth B of 1 Hz.

High-T_c frequency-selective Josephson detectors demonstrate the $DB^{1/2}$-values of more than 10^5 at the junction temperature of 80 K [22]. Previously, to characterize CW radiation sources with HTSA [12], we used narrow bandwidths B of (1÷100) Hz, and an extended dynamic power range of four-five orders was available, allowing for high signal/noise ratios in the response measurements. In the THz measurements of 1μs-pulses, a Josephson detector needs the post-detection bandwidth $B \approx 1$ MHz. Therefore, the dynamic power range of the detector, together with the maximally available signal/noise ratio, decreases to $\approx 10^2$. This circumstance complicates the characterization of the THz radiation with HTSA and requires additional noise reduction procedures of the measured signals. Among the various tested techniques, we have chosen the FFT low-pass filtering for this purpose.

B. Spectral resolution and spectral range

Voltage fluctuations result in the frequency modulation of the Josephson oscillations and corresponding broadening of their linewidths δf. This effect imposes a fundamental limitation on the spectral resolution of Josephson frequency-selective detectors and HTSA. In the case of wideband fluctuations with the cutoff frequency $f_{max} >> \delta f$, the spectrum of Josephson oscillations near the fundamental frequency f_j has a Lorentzian line shape, while the shape is Gaussian in the case of low-frequency fluctuations with $f_{max} << \delta f$ [23]. Thermal fluctuations of currents with the spectral density $S_I(f) = 2kT/R_n$,

results in the following Josephson linewidth δf

$$\delta f = \frac{1}{2\pi}\left(\frac{2e}{h}\right)^2 S_v(0) = \delta f_0\left(1+\frac{3f_c^2}{2f_j^2}\right), \quad (3)$$

where $S_v(0) = (dV/dI)^2\ [S_I(0) + S_I(f_j)(I_c^2/2I^2)]$ is the spectral density of voltage fluctuations in JJ including a down-conversion term $S_I(f_j)(I_c^2/2I^2)$, $dV/dI = R_n(f_j^2+f_c^2)^{0.5}/f_j$ is the differential resistance of JJ and $\delta f_0 = 4\pi(2e/h)^2kTR_n$ is the Josephson linewidth in an ideal case at large $f_j >> f_c$, but without additional noise contributions [23]. Here, in the brackets of (3), one can see a combined effect of rising differential resistance $dV/dI = R_n(f_j^2+f_c^2)^{0.5}/f_j$ and increasing contribution of the down-conversion term $S_I(f_j)(I_c^2/2I^2)$ to the enhancement of the linewidth with the decrease of the frequency $f_j < f_c$.

When the Josephson frequencies $f_j=2eV/h$ are in the THz range, the energy eV corresponds to a few millielectronvolts and is larger than the thermal energy kT for junction temperatures below of few tens of K. In this case, nonequilibrium fluctuations are of importance, and the energy $eV/2$ should substitute the thermal energy kT in the Nyquist formula for the spectral density $S_v(f)$ of voltage fluctuations in Josephson junctions [24]. Combining the effects of nonequilibrium current fluctuations, nonlinear I-V curve of JJ in RSJ model with the differential resistance $dV/dI > R_n$ and down-conversion process of the fluctuations at Josephson frequencies to zero frequency, we get the following estimate of Josephson linewidth δf as a function of Josephson frequency f_j

$$\delta f = \delta f_0\left(1+\frac{3f_c^2}{2f_j^2}\right)\frac{f_j}{f_T}coth\left(\frac{f_j}{f_T}\right), \quad (4)$$

where $f_T = 4kT/h$ is the crossover Josephson frequency between the cases of thermal and nonequilibrium broadening of the linewidth in JJs. These two main parameters, f_c, and f_T, in (4) control the shape of the spectral dependence of Josephson linewidth $\delta f(f_j)$. As follows from the analysis of (4), the dependence δf vs. f_j has a minimum at Josephson frequency $f_{jm} \cong 1.8 f_c^{0.6} f_T^{0.4}$.

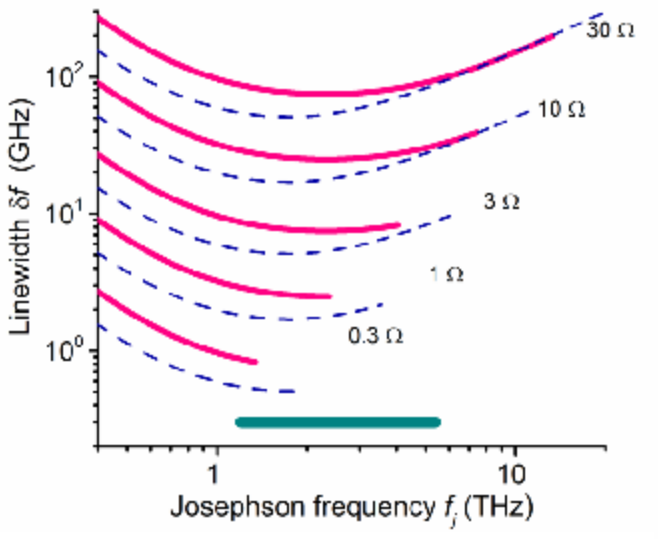

Fig. 1. Josephson linewidth δf as the function of Josephson frequency f_j for typical [001]-tilt $YBa_2Cu_3O_{7-x}$ bicrystal junctions at the temperature of 5K (dashed line) and 50 K (solid line) according to Eq. (4). The spectral ranges of each $\delta f(f)$-dependences are up to the maximum frequencies f_m determined by Joule heating in the junctions with various resistances R_n. A thick straight line below shows the total spectral range of QCLs.

Fig. 1 shows the Josephson linewidths δf vs. Josephson frequencies f_j calculated from (4) for [001]-tilted $YBa_2Cu_3O_{7-x}$ bicrystal junctions with the crossover frequencies f_T of 0.42 THz (T = 5 K, dashed lines) and 4.2 THz (T = 50 K, solid lines). We have used the typical average values of the characteristic voltages I_cR_n of 2.8 mV (f_c = 1.4 THz) at 5 K and 1.2 mV (f_c = 0.6 THz) at 50 K for these JJs with the normal-state resistances R_n from 0.3 Ω to 30 Ω. The $\delta f(f_j)$-dependence for JJ at 5 K with R_n =30 Ω (a dashed line) is presented in the full spectral range of (0.4 ÷ 20) THz. At low frequencies, it goes down with the increase of the frequency f_j, reaches the minimum at f_j =1.72 THz, and then increases.

Similar behavior one can see for the same JJ with R_n = 30 Ω at 50 K (a solid line), but with the minimum at a higher frequency f_j = 2.32 THz. In spite of the ten-fold decrease of the temperatures of JJ from 50K to 5 K, the minimum value of Josephson linewidth δf decreases only slightly, from 75 GHz to 51 GHz. A similar situation is in Fig.1 for all JJs with resistances R_n from 0.3 to 30 Ω. This finding shows that the decrease of the temperatures of the typical $YBa_2Cu_3O_{7-x}$ bicrystal JJs has a rather moderate effect on Josephson linewidth. More than a two-fold increase in the characteristic Josephson frequency $f_c(T)$ and a ten-fold decrease of the crossover frequency f_T practically compensate the ten-fold decrease of δf_0 in Eq.(4).

The plotted curves $\delta f(f_j)$ are inside the spectral ranges of the ac Josephson effect in the typical $YBa_2Cu_3O_{7-x}$ bicrystal JJs at given values of temperatures and resistances. At the high-frequency end of the Josephson spectrum, Joule heating of JJs with the dc power $P = (hf_j/2e)^2/R_n$ may be comparable with some critical value P_0, and intensities of Josephson oscillations may show an exponential decrease ~ $\exp(P/P_0)$ for higher f_j [25]. We use the P_0-values of 12.5 μW for junction temperature of 50K and 28 μW for T = 5 K, which we get from the measured THz responses of [001]-tilt $YBa_2Cu_3O_{7-x}$ bicrystal junctions [19].

We calculate the maximum frequencies f_m in each curve of Fig. 1 using the following criterion $(hf_m/2e)^2/R_n = 2P_0$. This approach gives a very good fit to the values of f_m for high-T_c JJs obtained from CW THz measurements [12], [19], and [26]. For example, the JJ with R_n = 0.37 Ω at T = 62 K demonstrated the Josephson linewidth δf of 1 GHz at the maximum frequency of 1.48 THz [12], while the JJ with R_n of 7 Ω at 35 K showed δf of 25 GHz up to 4.25 THz [26].

A set of dependencies $\delta f(f)$ for various temperatures and resistances (Fig. 1) helps us to choose the proper JJ for HTSA with the required spectral resolution and spectral range. In this work, we plan to use [001]-tilt $YBa_2Cu_3O_{7-x}$ bicrystal junctions for spectral characterization of the QCLs, which operate in the range from 1.2 to 5.4 THz (shown in Fig. 1 by a thick straight

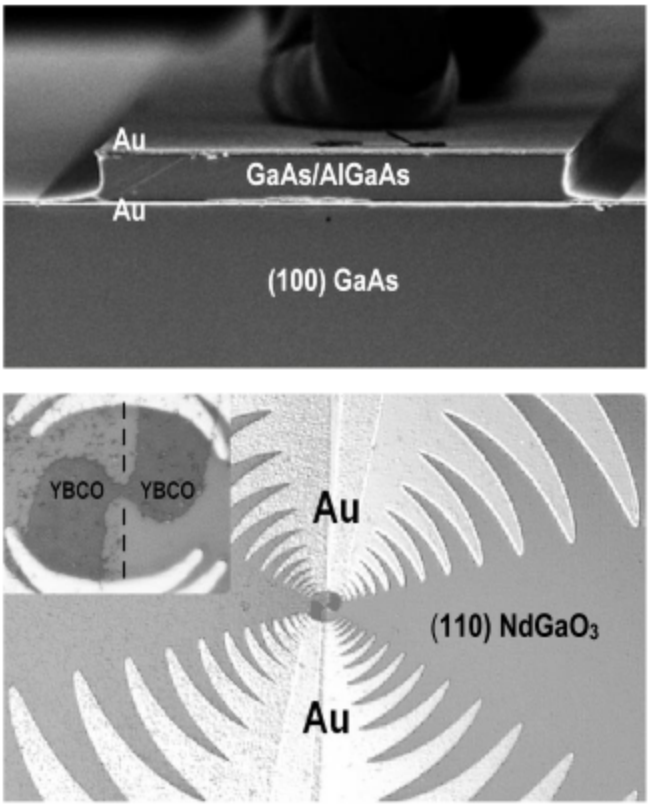

Fig. 2. Upper panel: 97×135 μm² SEM image of QCL with an active area of 10×100 μm². Lower panel: 145×520μm² optical image of Au log-periodic sinuous antenna with Josephson junction in the apex. Inset: 35x35μm² optical image of $YBa_2Cu_3O_{7-x}$ (YBCO) Josephson junction with a bicrystal boundary in the 2×11.3° (110) $NdGaO_3$ substrate shown by a dashed line.

line). Then, according to Fig. 1, we may choose the JJ with the R_n-values in the range of (5 ÷ 10) Ω and expect the minimum spectral resolution of around (13 ÷ 25) GHz at $T = 50$ K.

III. Experiment

A. Set-up

We have used THz QCLs with an active region based on four tunnel-coupled quantum wells GaAs/$Al_{0.15}Ga_{0.85}As$ with a resonant-phonon depopulation scheme [27]. The QCL heterostructure consisting of 222 periods are grown by molecular beam epitaxy on semi-insulating (100) GaAs substrates under arsenic-stabilized conditions. Fig. 2 (an upper panel) shows the SEM cross-section of one of the QCLs under study. The active GaAs/$Al_{0.15}Ga_{0.85}As$ area of the QCL has a width of 100 μm and a height of 10 μm. We use conventional processing [28] for the fabrication of a double Au–Au metal waveguide with the length of 2.5 mm.

To fabricate high-T_c Josephson junctions, we use epitaxial growth of (001) $YBa_2Cu_3O_{7-x}$ thin films on (110) $NdGaO_3$ bicrystal substrates [29]. The inset in the lower panel of Fig. 2 shows an optical plane-view image of $YBa_2Cu_3O_{7-x}$ (YBCO) thin-film electrodes and a 1.5μm-wide YBCO bridge crossing a bicrystal boundary on the 2×11.3° (110) $NdGaO_3$ substrate. An integrated Au log-periodic sinuous antenna improves the electromagnetic coupling of these JJs with THz radiation. The lower panel of Fig. 2 shows a corresponding optical image of

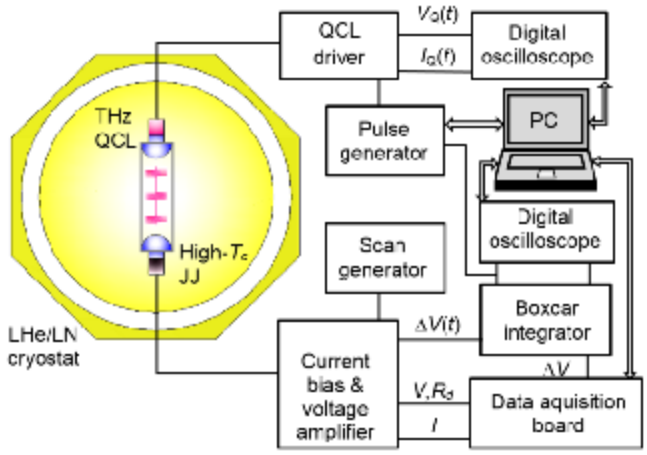

Fig. 3. Experimental setup with a quantum cascade laser (QCL) as a pulsed THz source and a high-T_c Josephson junction (JJ) as a detector in a liquid helium/liquid nitrogen (LHe/LN) cryostat.

the antenna in reflected light. In this work, Josephson junctions with the resistances R_n from 7 to 43 Ohms, and characteristic voltages I_cR_n (50 K) ≥ 1 mV are under study.

Fig. 3 shows a diagram of the experimental set-up. We mount a QCL on an oxygen-free-copper holder using an indium foil and attach a hyperhemispherical sapphire lens to the emitting facet of the QCL. The QCL holder is on a cold plate of a cryostat HDL-5 [30] filled with liquid helium or nitrogen (LHe/LN cryostat). Pulsed THz radiation from the QCL propagates to a high-T_c Josephson junction, which is on the same cold plate of the cryostat as the QCL and with a similar sapphire lens. A thin-wall stainless steel tube surrounds the space between the lenses to reduce radiation losses of highly diverged QCL radiation. Both the QCL and the high-T_c JJ are standing in a vacuum chamber of a cryostat, thus avoiding possible distortions of the spectra associated with THz losses in atmospheric air. To reach the cold-plate temperatures as low as 50 K, we have pumped liquid nitrogen in the cryostat with a membrane pump.

A self-made pulse driver delivers a train of current pulses $I_Q(t)$ to the QCL with a repetition time of 2 ms. A pulse generator controls the variation of the pulse peak values. The pulse driver delivers the pulse signals proportional to the $I_Q(t)$ and the voltage pulses $V_Q(t)$ on a QCL to a digital oscilloscope.

When operating in the same cryogenic environment, the QCL- and JJ-circuits have a finite electromagnetic coupling. Therefore, the current QCL pulses with 1A-amplitudes and sub-microsecond fronts affect the dc and signal characteristics of the JJ significantly. This circumstance is the main difficulty in spectral measurements of QCL radiation with Josephson junctions in the same cryogenic environment. A set of measures, including shielding, symmetrical wiring, and filtering, has helped us to decrease the interferences to a reasonable level.

Fig. 4a shows the current pulse $I_Q(t)$ with the maximum value $I_{Qmax} = +1.45$ A and the corresponding voltage pulses $V_Q(t)$ for a typical QCL under study. The pulse widths of $I_Q(t)$ is of 2 μs, and the leading and trailing edges of the pulse are close to

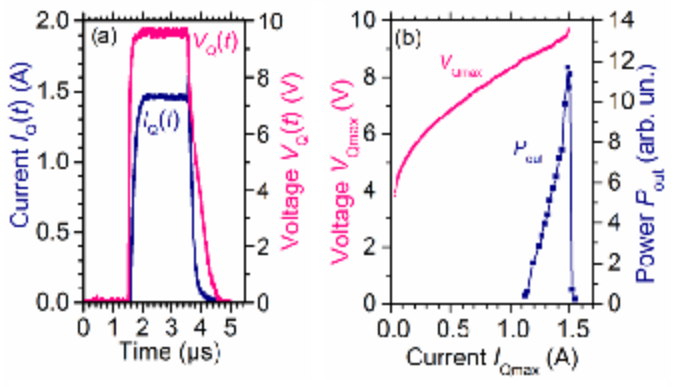

Fig. 4. (a) Pulse forms for a typical QCL under study: a current pulse $I_Q(t)$ with a maximum value I_{Qmax} of 1.45 A and a corresponding voltage pulse $V_Q(t)$. (b) *V-I* curve (solid line) of the QCL from pulse measurements at $T = 51$ K and output QCL power P_{out} measured by a pyroelectric detector vs. the QCL current I_{Qmax} (squares, a thin line is a guide to the eye).

exponential functions with a time constant τ of 120 ns. The *V-I* curve of QCLs is measured, starting from the corresponding driver signals. The driver increases the peak I_{Qmax} of the pulses $I_Q(t)$ from zero to 1.5 A, and the oscilloscope records the peak values of $V_Q(t)$ as a *V-I* curve. The time interval of (200-500) ns before the trailing edge of the $I_Q(t)$-pulse is preferable to measure these maximum current and voltage values and to exclude the impact of transient processes. Fig. 4b shows the resulting *V-I* curve for a typical QCL. The QCL's average output power, measured separately by a pyroelectric detector, develops at a threshold value of I_Q near 1.1 A. As the current I_Q increases, the radiation power P_{out} increases, reaching a maximum value before the instability points at the I_Q-values of around 1.5 A.

The JJ is current-biased, and a differential preamplifier delivers the signals directly proportional to the junction voltages. The current I through the JJ is scanned by a scan generator so that Josephson frequencies $f_J = 2eV/h$ are in the range of interest for spectral analysis. A data acquisition board (see Fig. 3) digitizes the signals proportional to the current bias I, the DC voltage V, and the differential resistance $R_d(I)$ of the JJ.

In the set up (Fig. 3), we use a digital oscilloscope to visualize the responses $\Delta V(t)$ of the JJ to pulsed THz QCL radiation, an analog boxcar integrator to record, and a data acquisition board to digitize them. A personal computer (PC) with the developed software controls the QCL pulse bias circuit with data acquisition from the QCL driver and electronics of the JJ. We have found that the best signal-to-noise ratio for measuring the response of JJs is at the end of the driving laser pulse when all transients from the leading edge of this driving pulse relax. Correspondingly, we have adjusted the time position of the gate pulse in the boxcar integrator under visual control with the digital oscilloscope.

A set of Shapiro current steps at the voltages $V_n = nhf_1/2e$ ($n = 1, 2, 3\ldots$), which appear on the *I-V* curves of JJs under intensive monochromatic radiation with the frequency f_1 , is a standard mean for voltage (and Josephson frequency) calibration [23]. We have used the radiation of an optically-pumped HCOOH laser with a specific spectral line of the well-defined value $f_1 = 692.9514$ GHz [31], [32] and assigned the values of dc voltages V_n of several Shapiro steps to values of $nhf_1/2e$.

With this calibration, the dc voltage and frequency accuracy in HTSA might be as high as that of the table frequencies in the absence of voltage fluctuations in JJs. If intrinsic thermal voltage fluctuations with the root mean square value $\langle V_n^2\rangle^{0.5} = (4kTR_nB)^{0.5}$ dominate in JJs, the voltage and frequency accuracy might be as low as 0.2 μV and 100 MHz in the case of the JJ with R_n of 10 Ω at $T = 50$ K and $B = 1$ MHz. In spectral measurements of QCL radiation with JJs, residual low-frequency voltage fluctuations induced by interferences from the pulsed QCL-circuitry affect the accuracy of the dc voltage (and frequency) measurements. Nevertheless, this calibration gives a rather good relative frequency accuracy of 3.5×10^{-4} and the absolute frequency accuracy of 1 GHz at a frequency of 2.2 THz.

B. Results

Fig. 5a demonstrates the *I-V* curve and the differential resistance R_d vs. V for one of the JJs with $R_n = 7$ Ω and $I_cR_n = 1.1$ mV at $T = 51$ K. The *I-V* curve of the JJ is of more than three orders lower magnitudes of current and voltage in comparison with that of the QCL (Fig. 4b). Nevertheless, we have measured the static electrical characteristics $I(V)$ and $R_d(V)$ with the accuracy required for HTSA, which shows good suppression of

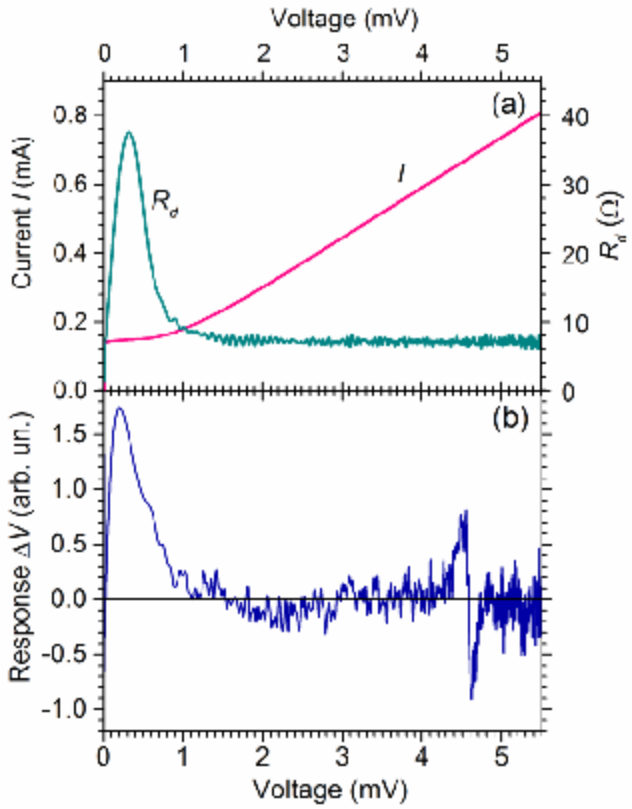

Fig. 5. (a) *I-V* curve and differential resistance R_d vs. voltage V of a $YBa_2Cu_3O_{7-x}$ bicrystal junction with $R_n = 7$ Ω at $T = 51$ K. (b) Response ΔV vs. V of the same JJ to QCL radiation with the pulsed current, as in Fig. 4a.

the interferences from QCL drive circuits. The $R_d(V)$-dependence has a maximum at the voltage $V_m = 326$ μV, and at higher voltages, shows oscillating behavior due to interaction of Josephson radiation with intrinsic resonances in the log-periodic antenna and the immediate environment of JJ. At the voltages higher 3 mV, noisy behavior around an average value R_n of 7 Ω gradually replaces the regular oscillating pattern in $R_d(V)$.

Fig. 5b shows the response $\Delta V(V)$ of the same JJ with $R_n = 7$ Ω at $T = 51$ K to QCL radiation. The response demonstrates a well-developed odd-symmetric resonance with a center near the voltage of 4.6 mV, and a peak at the voltage of 205 μV. The first resonance is due to the frequency pulling of Josephson oscillations in the JJ by high-frequency external narrowband radiation from the QCL. The low-voltage peak in the response $\Delta V(V)$ is due to another detection mechanism in JJ, i.e. suppression of the critical current by the same radiation, and it should be proportional to $R_d(V)$ at low voltages. However, here, the maximum of $\Delta V(V)$ is lower than the maximum of $R_d(V)$, and this is a hint that low-frequency components are present in QCL radiation. JJs detect radiation with the frequencies f, which are lower than the enhanced Josephson linewidth δf at low voltages, in a classical detection mode, where $\Delta V(V)$ is proportional to the second derivate d^2V/dI^2 vs. V and the maxima of the responses for lower frequencies are always shifted to lower voltages than that of for high-frequencies [33].

The responses of several JJs to QCL radiation demonstrate this low-voltage shift of the maxima and even negative responses of some JJ at the intermediate voltages due to a negative sign of the d^2V/dI^2 vs V there. Probably, these low-frequency components are due to the down-conversion processes inside a QCL cavity, when the radiation from several modes with close frequencies mix and produce some low-frequency background.

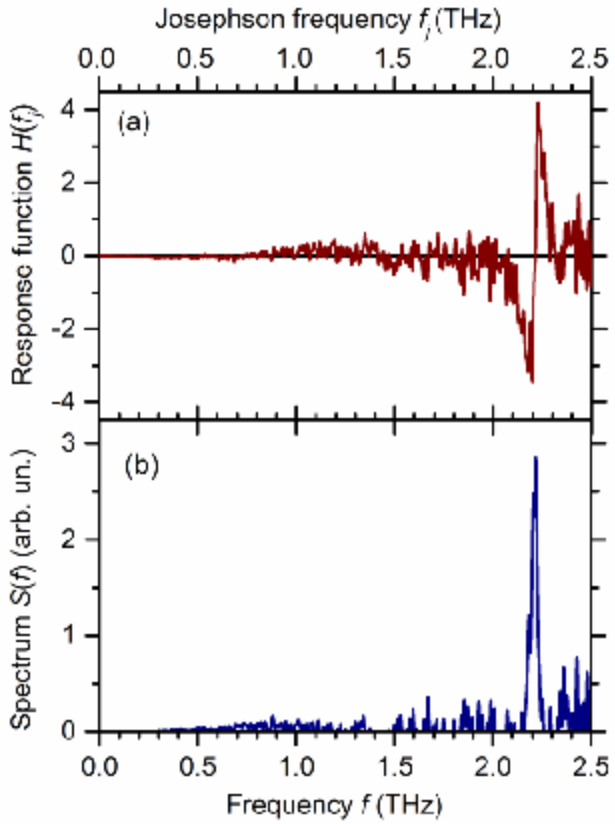

Fig. 6. (a) Normalized response function $H(f_J)$ obtained according to (2) from the experimental data (Fig. 4). (b) Spectrum $S(f)$ of radiation from a QCL recovered from $H(f_J)$ according to (1).

According to (2) and the relation $\Delta I(V) = -\Delta V(V)/R_d(V)$, we have converted the experimental data V, $I(V)$, $R_d(V)$, and the response $\Delta V(V)$ from Fig. 5 to the normalized response function $H(f_J)$. Fig. 6a demonstrates the result. A resonance feature is found in the function $H(f_J)$ near the frequencies $f_J \cong 2.2$ THz. Using the inverse Hilbert transform according to (1), we recover the double-sided spectrum $S(f)$ of QCL radiation from the detector response function $H(f_J)$ for positive and negative frequencies f_J. Fig. 6b shows the result for the positive frequencies. The spectrum shows some noise components, which increase with the frequency and interfere with the spectrum recovery. We have used an additional noise reduction procedure based on low-pass FFT filtering up to the level when the maximum in the spectrum starts to decrease. The spectrum contains a line at the frequency f near 2.2 THz with a linewidth of 35 GHz.

Fig. 7 shows a more detailed view of the spectrum $S(f)$ (a solid curve 1) in the reduced frequency range near the detected spectral line. The shape of the line looks rather asymmetric. The observed linewidth is broader than the Josephson linewidth δf of 17 GHz estimated from (4) for the junction parameters at the temperature of 51 K. To explain an excess width of the measured spectral line, we cannot exclude the effect of additional voltage modulation on JJ due to the interference

TABLE I.

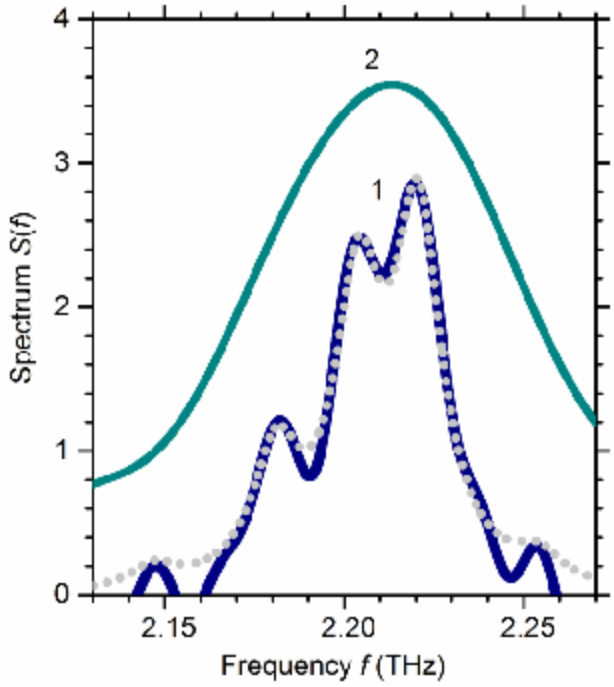

Fig. 7. Spectra $S(f)$ (solid lines) of QCL measured with $YBa_2Cu_3O_{7-x}$ bicrystal JJs with $R_n = 7$ Ω (curve 1) and $R_n = 43$ Ω (curve 2). Dots show a result of nonlinear fitting of the curve 1 by five Lorentz curves with various frequencies f_j and the same width Δf.

CENTRAL FREQUENCIES AND RELATIVE INTENSITIES OF LORENTZ LINES USED IN NONLINEAR FITTING OF QCL SPECTRUM

Index i	Central frequency f_i, THz	Relative intensities A_i	Mode assignment
1	2.147	0.06	
2	2.181	0.35	TM_{01}
3	2.204	0.78	TM_{00}
4	2.221	1	TM_{00}
5	2.254	0.08	

pulses from the QCL current drive. However, if it were the case, the form of a spectral line would be more close to the symmetrical Gaussian curve. Furthermore, the line contains some internal structure, which looks like a set of resonances with various frequencies.

We have applied nonlinear fitting of the sum of five Lorentz curves of the same linewidth Δf to the obtained spectrum $S(f)$ and Fig. 7 shows the result in dots. The value of Lorentz linewidths Δf for the best fit is (16 ± 1) GHz. Table I shows a set of central frequencies and intensities, which we have obtained as the best fit. In a central part of a spectrum, there is a good coincidence between the HTSA spectrum (a solid line 1) and the fitted curve (dots). The lines at the frequencies f_2, f_3, and f_4 have the largest intensities and fit better than the weak lines at the frequencies f_1 and f_5.

The value of Δf of (16 ± 1) GHz obtained from the fitting procedure is close to the Josephson linewidth δf = (17.0 ± 0.5) GHz estimated from (4) for JJ with R_n = 7 Ω at 51 K. That means that intrinsic fluctuations do broaden the Josephson linewidth in JJ, but not external interferences. To get an additional proof of this conclusion, we have carried out similar experiments with the JJs with much higher resistances *Rn*, so that their Josephson linewidths are larger than the total spectral width of the QCL operating at several resonator modes.

Fig. 7 shows the spectrum (a solid line 2) of the same QCL at the same current bias, which is measured by the $YBa_2Cu_3O_{7-x}$ bicrystal JJ with the characteristic voltage I_cR_n = 1.1 mV and the resistance R_n = 43 Ω at T = 50 K. The spectrum has a maximum at the frequency of (2.214 ± 0.001) THz. The shape of the spectrum in Fig. 7 is more symmetrical, and the linewidth Δf is of around 90 GHz. The measured linewidth of the spectrum 2 is close to the value of Josephson linewidth δf = (102 ± 5) GHz calculated from (4) for the JJ parameters used in the measurements. A 10%-decrease of the measured linewidth compared with values of pure thermal broadening might be due to the emerging effect of capacitance shunting at high resistance values [23]. Thus, HTSA measures QCL radiation with the spectral resolution determined by the intrinsic Josephson linewidth of the high-T_c JJs.

IV. DISCUSSION

Conventional THz QCLs emit at the frequencies corresponding to the Fabry-Perot modes of the QCL active volume confined between Au-electrodes. The measurements of THz radiation from our QCLs with Fourier spectroscopy [27] show the spectra consisting of a few intensive spectral lines with the same spacing around 16 GHz. This spacing is close to the value of $c/2nL$ = 18 GHz calculated for the longitudinal modes of the QCL with the length L = 2.5 mm and the effective refractive index n = 3.3. Therefore, we may suppose that the internal structure of the recovered spectrum in Fig. 7 is the result of the QCL operation on some most intensive modes and the widening of the JJ response by a finite Josephson linewidth. Asymmetry of the obtained spectrum may be due to the various intensities of the modes.

Indeed, the difference f_4 - f_3 of 17 GHz and the relative intensities A_3 and A_4 are very close to those of the most intensive lines in the spectra, measured earlier by Fourier spectroscopy [27]. However, the frequency difference $f_3 - f_2$ is of 23 GHz and, the intensity A_2 of the line is much higher when compared with the rest of the lines in the spectra, measured earlier [27]. These circumstances indicate that the line with frequency f_2 belongs to another set of resonances in the active volume of the QCL, which we have failed to detect with Fourier spectroscopy earlier.

Due to the interferometric principle and a corresponding increase of the frequency errors with the angle of incoming radiation, Fourier spectroscopy operates effectively at small solid angles [6]. When THz radiation comes to the Fourier spectrometer along the direction normal to the QCL facet, the radiation from the TM_{00} group of the longitudinal modes is mainly detected [8]. The Fourier spectrometer in the off-normal configuration mainly detects THz radiation from higher modes of the QCL resonator. The measurements show that the 150μm-wide QCL emits 3.6THz-radiation from the TM_{01} mode in the directions at the angle of 25° [8].

In HTSA, which operates in the frequency domain, there is no limitation on the angles of incoming radiation, and it detects all spectral components without changing the geometry of the measurements. The set-up for the measurements with HTSA includes two hyperhemispherical lenses with a light pipe between the QCL and the JJ (see Fig. 3), and this optical configuration collects radiation in a broad angular range. Thus, HTSA may characterize THz radiation from the QCLs in one run in more detail, including an extended set of the longitudinal and transverse modes, compared with a similar study with Fourier spectroscopy.

Using the results of [8] and [27], we can conclude that the most intensive lines at the frequencies f_3 and f_4 belong to the TM_{00} longitudinal modes, and the line at the frequency f_2 belongs to the TM_{01} modes. The weak line at the frequency f_1 is below the frequency f_2 on 34 GHz that is equal to double frequency spacing $c/2nL$, and this line presumably belongs to the same group of the resonator modes as the line at f_2. Another weak line at f_5 is of 33 GHz higher than the strong line at f_4 and, presumably, belongs to the same group of resonator modes, which are the TM_{00} modes. We consider the assignment of the weak lines as very preliminary and put only the strong lines in the corresponding column of Table I.

Here, we use the [001]-tilt $YBa_2Cu_3O_{7-x}$ bicrystal JJs fabricated by epitaxial growth of the c-axis $YBa_2Cu_3O_{7-x}$ thin films. Their characteristic voltages I_cR_n are in the range from 1 to 2 mV at the temperatures between 50 and 5 K, and their

characteristic Josephson frequencies $f_c \leq 1$ THz are lower than that required for optimal detection of QCL radiation. The resistances R_n of these junctions are high, and it is desirable to decrease their values to reach narrower intrinsic Josephson linewidths, even for lower Josephson frequencies.

Therefore, to improve the resolution and the spectral range of the HTSA for QCL studies, one should employ Josephson junctions of lower resistances R_n and higher I_cR_n-values. The first HTSA measurements of CW THz CH_3OH laser radiation using [100]-tilted $YBa_2Cu_3O_{7-x}$ bicrystal junctions with high I_cR_n and low resistances demonstrate promising results [12]. More precise tuning of the resistance and temperature values according to (4) and Fig. 1 might be required.

V. Conclusion

In summary, we have demonstrated the potential of Hilbert-transform spectral analysis with high-T_c Josephson frequency-selective detectors for characterization of THz radiation from pulsed quantum cascade lasers in the same cryogenic environment. We have considered the limitations on the operation of this type of spectral analysis imposed by nonequilibrium voltage fluctuations and Joule heating in Josephson junctions.

The spectrum of QCL emission recovered by HTSA consists of several lines at the frequencies around 2.2 THz, which are due to the excitation of a variety of resonant modes in the active volume of the QCL. The frequency spacing between the longitudinal modes and their relative amplitudes agree with the corresponding parameters in emission spectra of the same QCLs measured by Fourier-transform spectroscopy. We have found that, due to a reduced power dynamic range and lower signal/noise ratios in the case of pulsed THz HTSA compared with those of in the case of CW THz HTSA, low-pass FFT filtering of experimental data is an essential part in spectrum recovery to reach the spectral resolution determined by the intrinsic Josephson linewidth.

This work paves the way to a more informative spectral analysis of novel QCLs and other THz sources in the frequency domain. Further work on optimization of HTSA operation with fine-tuning of the parameters of perspective high-*Tc* JJs is necessary and underway.

References

[1] M. Tounuchi, "Cutting-edge terahertz technology," *Nature Photon.,* vol. 1, pp. 97-105 (2007).

[2] M. A. Belkin, F. Capasso, "New frontiers in quantum cascade lasers: high performance room temperature terahertz sources," *Phys. Scr*., vol. 90, 118002 (2015)

[3] C. Sirtori, S. Barbieri, R. Colombelli. "Wave engineering with THz quantum cascade lasers", *Nature Photon*., vol. **7**, pp. 691-701 (2013)

[4] L. Bosco, M. Franckié, G. Scalari, M. Beck, A. Wacker, J. Faist, "Thermoelectrically cooled THz quantum cascade laser operating up to 210 K, " *Appl. Phys. Lett.*, 115, 010601 (2019).

[5] M. A. Kainz, et al., "Thermoelectric-cooled terahertz quantum cascade lasers," *Opt. Express,* vol. 27, 20688-20693 (2019)

[6] G.W. Chantry, *Submillimetre Spectroscopy*. London: Academic Press, 1971.

[7] A. J. L. Adam, et al., "Beam patterns of terahertz quantum cascade lasers with subwavelength cavity dimensions," *Appl. Phys. Lett*., vol. 88, 151105 (2006).

[8] S. Fathololoumi, et al., "Electrically switching transverse modes in high power THz quantum cascade lasers," *Opt. Express*, vol. 18, 10036 (2010)

[9] D. G. Paveliev, *et al*., "Experimental Study of Frequency Multipliers Based on a GaAs/AlAs Semiconductor Superlattices in the Terahertz Frequency Range," *Semiconductors*, vol. 46, pp. 121-125 (2012).

[10] B. D. Josephson, "Possible new effects in superconductive tunneling*", Phys. Lett.*, vol. 1, pp. 251-253 (1962).

[11] Yu. Ya. Divin, O. Yu. Polyanskii, A. Ya. Shul'man, "Incoherent radiation spectroscopy by means of the Josephson effect". *Sov. Tech. Phys. Lett.*, vol. 6, pp. 454-455 (1980).

[12] A. V. Snezhko, *et al.*, "Terahertz Josephson spectral analysis and its applications", *Supercond. Sci. Technol*., vol. 30, 44001 (2017).

[13] Yu. Ya. Divin, H. Schulz, U. Poppe, N. Klein, K. Urban, V. V. Pavlovskii, "Millimeter-wave Hilbert-transform spectroscopy with high-T_c Josephson junctions", *Appl. Phys. Lett*., vol. 68, pp. 1561-1563 (1996)

[14] E. Kume, I. Iguchi, and H. Takahashi, "On-chip spectroscopic detection of terahertz radiation emitted from a quasiparticle-injected nonequilibrium superconductor using a high-T_c Josephson junction", *Appl. Phys. Lett*., vol. 75, pp. 2809–2811 (1999).

[15] Y. Y. Divin, et al., "Hilbert-Transform Spectroscopy with High-T_c Josephson Junctions: First Spectrometers and First Applications", *IEEE Trans. Appl. Supercond*., vol. 9, pp. 3346-3349 (1999).

[16] W. W. Xu, J. Chen, L. Kang, and P. H. Wu, "Extraction of the spectral information of terahertz signals using superconducting Josephson junction", *Sci. China Tech. Sci.,* vol. 53, pp. 1247−1251 (2010).

[17] R. Kaneko, I. Kawayama, H. Murakami and M. Tonouchi," Detection of Pulsed Terahertz Waves Using High-Temperature Superconductor Josephson Junction", *Appl. Phys. Express*, vol. 3, 042701 (2010).

[18] D. Y. An et al., "Terahertz emission and detection both based on high-T_c superconductors: Towards an integrated receiver," *Appl. Phys. Lett*., vol. 102, 092601 (2013).

[19] Y. Y. Divin, U. Poppe, O. Y. Volkov, and V. V. Pavlovskii, "Frequency-selective incoherent detection of terahertz radiation by high-T_c Josephson junctions", *Appl. Phys. Lett.*, vol. 76, pp. 2826-2829 (2000).

[20] Y. Y. Divin, et al., "Classical and Josephson detection of terahertz radiation using YBa2Cu3O7-x [100]-tilt bicrystal junctions." *J. Phys.: Conf. Ser*., vol. 43, pp.1322-1325 (2006).

[21] V. Shirotov, et al., "Application of Hilbert spectroscopy to pulsed far-infrared radiation,"IEEE Trans. Appl. Supercond., vol. 13, pp. 172-175 (2003)

[22] V. V. Shirotov and Y. Y. Divin, "Frequency-Selective Josephson Detector: Power Dynamic Range at Subterahertz Frequencies," Techn. Phys. Lett., vol. **30**, pp. 522–524 (2004).

[23] K. K. Likharev, "Dynamics of Josephson Junctions and Circuits," (Gordon and Breach, New York, 1986), Chap.4.

[24] A. I. Larkin and Yu. N. Ovchinnikov, "Radiation line width in the Josephson effect," *Sov. Phys. JETP*, vol.26, pp.1219-1221 (1968).

[25] M. Tinkham, M. Octavio, and W. J. Skocpol, "Heating effects in high-frequency metallic Josephson devices: Voltage limit, bolometric mixing, and noise," J. Appl. Phys., vol. 48, pp.1311- 1320 (1977).

[26] Y. Y. Divin, O. Y. Volkov, V. V. Pavlovskii, U. Poppe, K. Urban, "Terahertz spectral analysis by ac Josephson effect in high-*Tc* bicrystal junctions," IEEE Trans. Appl. Supercond., vol. 11, pp.582-585 (2001).

[27] R. A. Khabibullin, et al., "The operation of THz quantum cascade laser in the region of negative differential resistance," *Opto-Electronics Review*, vol. 27, pp. 329-333 (2019).

[28] A. V. Ikonnikov et al., "Terahertz radiation generation in multilayer quantum-cascade heterostructures," *Tech. Phys. Lett.,* vol. 43, pp. 362–365 (2017).

[29] Y. Y. Divin, U. Poppe, I. M. Kotelyanskii, V. N. Gubankov, and K. Urban, "Terahertz Spectroscopy Based on High-T_c Josephson Junctions," *J. Commun. Technol. Electron*., vol. 53, pp.1137-1152 (2008).

[30] [Online].Available:http://www.infraredlaboratories.com/HDL_Series_Dewars.html

[31] G. Kramer and C. O. Weiss, "Frequencies of Some Optically Pumped Submillimetre Laser Lines," *Appl. Phys*., vol. 10, pp. 187-188 (1976).

[32] T. Hori and N. Hiromot, "Characteristics of a far-infrared molecular laser optically-pumped by a high-power CO_2 laser", *Int. J. Infrared Milli. Waves*, vol. 13, pp. 483–496 (1992).

[33] V. V. Pavlovskiy, I. I. Gundareva , O. Y. Volkov, and Y. Y. Divin, "Wideband detection of electromagnetic signals by high-T_c Josephson junctions with comparable Josephson and thermal energies," *Appl. Phys. Lett*., vol. 116, 082601 (2020).

In Situ Hilbert-Transform Spectral Analysis of Pulsed Terahertz Radiation of Quantum Cascade Lasers by High-T_c Josephson Junctions

Oleg Volkov, Valery Pavlovskiy, Irina Gundareva, Rustam Khabibullin, and Yuriy Divin

Abstract—We have studied the applicability of high-T_c Josephson junctions (JJs) and Hilbert-transform spectral analysis (HTSA) for characterization of pulsed terahertz (THz) radiation. We have reconsidered the extension of HTSA into the THz range, including an impact of such emerging factors as nonequilibrium voltage fluctuations and dc Joule heating in high-T_c JJs, and found an unexpected weak temperature dependence of Josephson linewidth δf and a spectral dependence $\delta f(f)$ with a minimum. Due to this analysis, we have chosen $YBa_2Cu_3O_{7-x}$ bicrystal JJs for experimental study. The JJs have analyzed pulsed THz radiation from quantum cascade lasers (QCLs) located in the same cryogenic environment at 50 K. The spectra recovered by the JJ with R_n = 43 Ω consist of a line with a central frequency around 2.2 THz, which have a symmetrical form and the linewidth of 90 GHz close to the intrinsic Josephson linewidth of this JJ. The spectra measured by the JJ with R_n = 7 Ω and the intrinsic Josephson linewidth of 16 GHz consist of several lines at the frequencies f_i around 2.2 THz, which are due to the excitation of different resonant modes in the active volume of the QCL. The difference between the fitted central frequencies f_2 - f_1 of the strong lines and the ratio of their intensities are in agreement with the spectrum of the same QCL measured by Fourier spectroscopy. The developed technique paves the way for detailed and rapid characterization of pulsed THz sources in the frequency domain.

O. Volkov and V. Pavlovskiy are with the Kotelnikov Institute of Radio Engineering and Electronics, Russian Academy of Sciences, 125009 Moscow, Russia (e-mail: O_Volkov@cplire.ru and pvv@cplire.ru).

I. Gundareva was with the Peter Grünberg Institute (PGI-5), Forschungszentrum Jülich, 52425 Jülich, Germany, on leave from the Kotelnikov Institute of Radio Engineering and Electronics, Russian Academy of Sciences, 125009 Moscow, Russia. She is now with the Peter Grünberg Institute (PGI-9), Forschungszentrum Jülich, 52425 Jülich, Germany (I.Gundareva@fz-juelich.de).

R. Khabibullin is with the Mokerov Institute of Ultra High Frequency Semiconductor Electronics, Russian Academy of Sciences, 117105 Moscow, Russia (e-mail: khabibullin@isvch.ru).

Y. Divin is with the Kotelnikov Institute of Radio Engineering and Electronics, Russian Academy of Sciences, 125009 Moscow, Russia (e-mail: yyd@cplire.ru) and also with the Peter Grünberg Institute (PGI-5), Forschungszentrum Jülich, 52425 Jülich, Germany (Y.Divin@fz-juelich.de).